ELSEVIER

Tectonophysics 281 (1997) 173–193

TECTONOPHYSICS

Finite deformation and displacement fields on the southern Yemen margin using satellite images, topographic data and a restoration method

Frédéric Thoué [a,*], Gérard Vidal [a], Jean-Pierre Gratier [b]

[a] *Laboratoire de Sciences de la Terre, UMR-CNRS 5570, Ecole Normale Supérieure de Lyon, 46 Allée d'Italie, FR-69364, Lyon Cedex 07, France*

[b] *Laboratoire de Géophysique Interne et Tectonophysique, IRIGM, BP53x, FR-38041, Saint Martin d'Hères, France*

Received 27 September 1996; accepted 7 April 1997

Abstract

Geological interpretations of processed satellite images and structural field measurements were used to calculate the amount of extension and the finite displacement field of two stretched areas located on the northern margin of the Gulf of Aden, in Yemen. This calculation was done by a comparison between the deformed and the undeformed states of each studied area. The structural setting established from satellite-image interpretations and fieldwork yields a detailed geometry of the deformed state. The undeformed state was reconstructed from reference layers chosen on satellite images from folded and faulted geological markers. The strike and dip of those layers were computed directly from dip indicator measurements, identified on three-dimensional (3D) realistic views of the sites (derived from SPOT stereoscopic views and topographic data) and controlled by field measurements. From the previous structural data, a numerical model of the deformed state was prepared with respect to the structural setting. The two stretched areas were then restored to their undeformed state successively by (1) an unfolding method (use of the UNFOLD program on each folded piece bounded by faults), and (2) a best-fit method (fitting along the boundary of the unfolded pieces). The comparison between the deformed and undeformed states leads to quantifying the amount of strain and to establishing the total finite displacement field. The results point to differences in the amount of extension and in the finite displacement field between the two areas studied. Within the regional context of the Afar triple junction kinematics, this leads to the conclusion that there was an early extensional tectonic phase recorded on the southern Yemen margin, probably linked to the earlier opening of the Gulf of Aden.

Keywords: rifting; Yemen; satellite imagery; digital elevation model; strained structures restoration; displacement fields

1. Introduction

One of the major problems in tectonic studies is to test the compatibility of the geological and geophysical data in order (1) to quantify the deformation of a studied area, and (2) to establish the finite displacement field (relative to a fixed line). This displacement field may be compared with the local displacements deduced from other data (for example measurements on faults slickensides). By matching information on the displacements, it is possible by trial and error, to determine the best compatibility between all the data available in a given area.

* Corresponding author. Fax: +33 7272-8677; e-mail: thoue@geologie.ens-lyon.fr

PII S0040-1951(97)00071-1

We propose a method including successively (1) processing of satellite images and structural field measurements leading to the detailed geometry of the strain of a reference layer, (2) restoration of this deformed layer to its initial (undeformed) state, and then (3) calculation of the total finite displacement field, by a comparison of deformed and undeformed states, taking into account microtectonic field data from faults. This method thus calls for knowledge of both the deformed state and undeformed state of the studied area. Application of this method to the evolution of the southern margin of Yemen during Cenozoic times gives the amount of crustal extension and also reveals the detailed kinematics of the crustal blocks.

The deformed state of extensional areas is directly accessible and its geometry can be analysed and precisely described by satellite-image interpretations supplemented by fieldwork. Field measurements on slickensides of faults are used with inversion methods in order to complete the local structural setting.

The undeformed state of a deformed area may be reconstructed using several methods.

(1) Balanced geological cross-section techniques were first developed assuming that strain occurs without volume change (Dahlström, 1969; Hossack, 1979; Ménard, 1987; Mugnier et al., 1987). Even if some of these techniques combine several balanced cross-sections to produce a map of the initial state (DePaor, 1988), they consist only in a two-dimensional (2D) analysis of the strain.

(2) Palinspastic restoration of tectonic features consists of dividing the entire strained area into finite elements which are considered as homogeneous and continuous (Schwerdtner, 1977; Oertel and Ernst, 1978; Cobbold, 1979; Percevault and Cobbold, 1982; Gratier et al., 1989). Each element is restored to its initial state. By fitting these restored elements together, it is then possible to reconstruct the initial state of the deformed area. At a regional scale, these techniques allowed several authors (Percevault and Cobbold, 1982; Schultz-Ela, 1988; Gratier et al., 1989) to estimate displacement fields (relative to a fixed line). However, the techniques require areas of continuous strain, without accounting for their discontinuous part (major faults).

(3) Other techniques have been developed more recently, enabling folded and/or faulted layers to be restored (Barr, 1985; Mc Coss, 1988; Gratier et al., 1991; Rouby et al., 1993). These methods comprise different steps: (a) choice of a reference layer over the entire studied area; (b) numerical modelling of the geometry of the faulted and/or folded reference layer; (c) restoration of this layer to its undeformed state. Several methods have been developed for such restoration. Barr (1985) described a computer-based method for restoration of folded and faulted layer, but with a uniform extension direction. Mc Coss (1988) used folded lineations to unfold a folded area (without any fault). Least-square fitting was used by Audibert (1990) and Rouby et al. (1993) to restore faulted areas composed of rigid blocks. Finally, finite-element methods have been used for the restoration of folded and faulted areas (with non-cylindrical folds) (Gratier, 1988; Gratier et al., 1991; Gratier and Guillier, 1993).

Usually, the geological data used with this last group of techniques correspond to geological cross-sections, seismic profiles or deformation maps (Cobbold and Percevault, 1983; Guillier and Gratier, 1993; Rouby et al., 1993). In this paper, we present a new application of these restoration techniques using topographic data and digital satellite images supplemented by fieldwork. The amount of extension and the total finite displacements have been calculated in the southern Yemen margin, on one of the edges of the triple junction between the African, Arabian and Somali lithospheric plates. After a brief overview of the data used in this study, the methodology developed to model tilted blocks and to quantify extension is summarised. Then, the validity of these results is discussed according to the methodological limits and the regional kinematics of the Afar triple junction.

2. Structural setting of the southern Yemen margin

2.1. Geological context

The part of the southern Yemen margin surveyed in this study extends from about 43°E to 46°E in longitude and from 12°N to 14°N in latitude (Fig. 1). This continental margin lies at one of the edges of a triple junction involving two oceanic rifts (Red Sea and Gulf of Aden) and a continental rift (Afar rift) which corresponds to the northern part of the East

African Rift System. These rifts separate the African, Arabian and Somalian plates (Fig. 1a).

The geology of this margin (Fig. 1b) presents various types of sedimentary and volcanic rocks, from Proterozoic to Recent ages, which lie unconformably on a Panafrican basement. This basement mostly exhibits complex assemblages of metamorphic and crystalline rocks related to the Panafrican orogen (Geukens, 1960; Greenwood and Beackley, 1967) and strongly deformed as shown by the numerous isoclinal folds and shear zones. Few outcrops of Cambrian and Permian sediments are mainly described to the east and northeast of the margin (Greenwood and Beackley, 1967; Menzies et al., 1990; Davison et al., 1994). The Mesozoic sedimentary cover corresponds to marine series showing an increase of terrigenous components through times (Greenwood and Beackley, 1967; Menzies et al., 1990; Davison et al., 1994). The development of transpressional basins during Oxfordian times is the major tectonic activity reported during Mesozoic times (Tard et al., 1991). During Tertiary times, an important and predominantly alkaline volcanic series (Moseley, 1969; Chiesa et al., 1983) took place over about 40,000 km^2 to form the Yemen Traps Series (Geukens, 1960). Within this series, numerous basaltic dikes are observed (Moseley, 1969; Huchon et al., 1991; Mohr, 1991) and are well-developed in the lower part of the traps (Davison et al., 1994) as shown in Fig. 1b. Dike trends are oriented N120°E to N140°E in the southern part of Yemen (Moseley, 1969; Thoué, 1993) and mostly north–south in the northwestern part (Bohannon, 1989; Huchon et al., 1991; Mohr, 1991; Davison et al., 1994). It should be noticed that the traps outcrops vanish toward the east, at about 45°E.

2.2. Location of the studied areas along the margin

Two sectors were chosen to study the finite deformation of the margin and to quantify extension and displacement fields. Fig. 1b presents the precise location of these two surveyed areas. The first sector (sector of Umm Shatt) is located close to the Bab El Mandeb Strait which marks the limit between the Red Sea and the Gulf of Aden, whereas the second one (sector of Ba'tays) is located northeast of Aden, along the Gulf of Aden coast.

Those sectors are separated by an important structural trend striking N140°E and corresponding mostly to normal faults which cross the southern Yemen margin (Greenwood and Beackley, 1967; Grolier and Overstreet, 1978; Tard et al., 1991; Thoué, 1993). This N140°E trend running approximately from Aden to Dhala (Fig. 1b) corresponds to a wide major graben studied from a structural point of view by several authors (Huchon et al., 1991; Tard et al., 1991; Thoué, 1993) and also referenced as 'Dhala Graben' by Moseley (1969). This graben is interpreted as a transfer zone (Tard et al., 1991; Thoué, 1993) which separates crustal blocks along the margin as pointed out further east by Fantozzi (1996). The Yemen Traps Series outcrop to the west of this structural trend where the Umm Shatt area is located as well as the numerous plutons and dikes which intrude the volcanic and sedimentary cover (Moseley, 1969; Capaldi et al., 1987; Bohannon, 1989; Mohr, 1991; Menzies et al., 1992; Davison et al., 1994). East of this N140°E Aden–Dhala line where the Ba'tays area is located, no volcanic rocks linked to the Oligo–Miocene Yemen Traps Series occur on the Mesozoic sedimentary cover.

3. Geometry of the final state deduced from fieldwork and satellite imagery

3.1. Numerical data

Digital satellite images acquired by Landsat TM and SPOT satellites were used during this study to provide large-scale structural patterns of the deformed areas. The numerical scenes correspond to path and row 165-51 and 166-51 for Landsat TM and to K-J 146-324 and 149-323 for SPOT. The regions they cover on the southern Yemen margin are illustrated in Fig. 1a by light-grey shaded boxes for Landsat TM images and by dark-grey shaded boxes for SPOT images. SPOT scenes are in the panchromatic mode (10 m of ground resolution and a wide spectral band in the visible and near infrared part of the electromagnetic spectrum), whereas Landsat TM images are in the multispectral mode (30 m of ground resolution and seven narrow spectral bands from visible to thermal infrared). The SPOT scenes consist of stereoscopic couples (dark-grey shaded boxes in Fig. 1a) whose acquisition dates are respec-

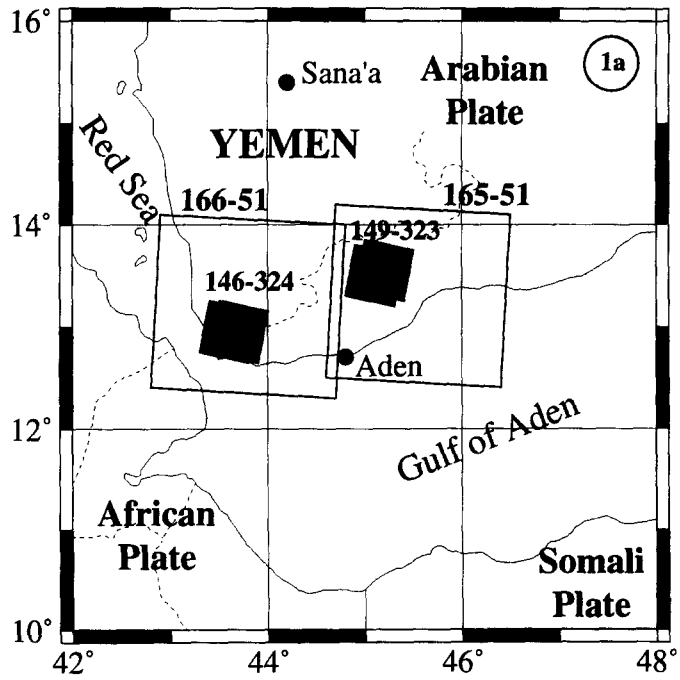
16°
14°
12°
10°
42°
44°
46°
48°
Sana'a
Arabian Plate
1a
YEMEN
Red Sea
166-51
165-51
149-323
146-324
Aden
Gulf of Aden
African Plate
Somali Plate

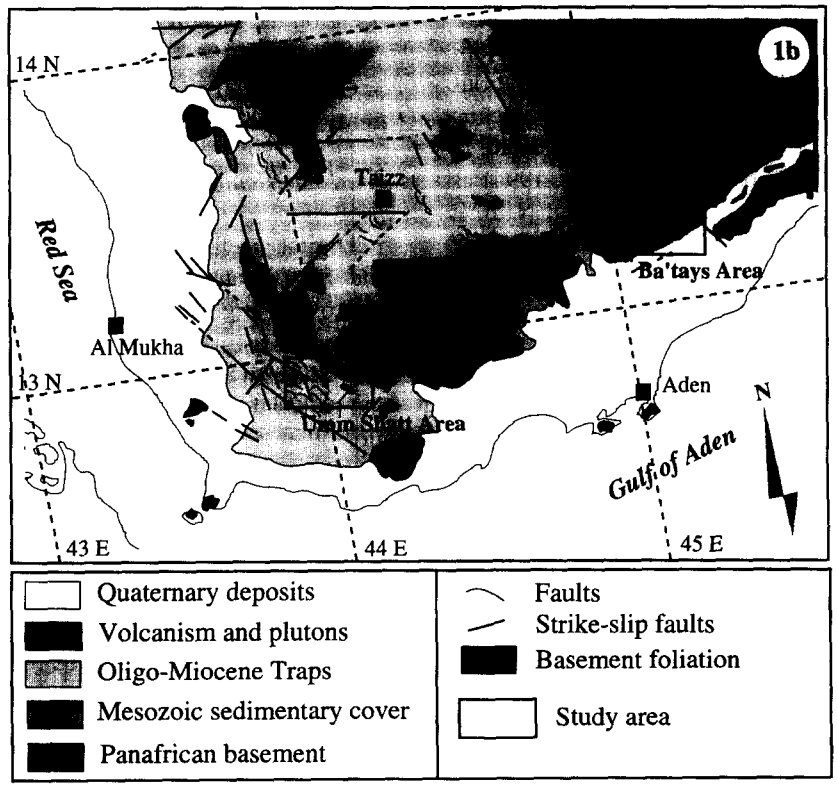
1b
14 N
13 N
Taizz
Red Sea
Ba'tays Area
Al Mukha
Aden
Gulf of Aden
N
43 E
44 E
45 E
Quaternary deposits
Volcanism and plutons
Oligo-Miocene Traps
Mesozoic sedimentary cover
Panafrican basement
Faults
Strike-slip faults
Basement foliation
Study area

tively 19/05/88 and 02/12/88 for the couple 146-323, 31/07/87 and 03/12/90 for the couple 149-323.

From the stereoscopic capabilities of each couple of SPOT images, Digital Elevation Models (DEM) were also computed using a program developed by the SINTEGRA/TIM3 laboratories at the University of Grenoble (Mémier, 1991). The DEM calculation yields a set of several millions of topographic points referenced by their (x, y, z) coordinates. These points are computed from the numerical correlation between the two images of each stereoscopic couple. The set of topographic points is processed to remove isolated abnormal elevations that appeared during the computation. These anomalies are due to random differences between the images (clouds or seasonal variations in the vegetation cover for example). This processed set is then sampled on a regular grid, with a square mesh, to obtain the final DEM. New images, so-called ortho-images, are then computed by removing both the planimetric and the elevation distortions of the oblique looking SPOT stereoscopic images and projecting these SPOT images onto the DEM regular grids. DEM and ortho-images are then superimposed to built three-dimensional (3D) perspective views of both the Umm Shatt and Ba'tays deformed areas. These perspective views as well as the satellite images will be used hereafter to precise the geometry of the final state of deformed areas.

3.2. Structural interpretative maps

Structural maps were built from the processed satellite images and improved by field data, allowing lithological limits, faults and dikes to be drawn respectively for the Umm Shatt area in Fig. 2a and the Ba'tays area in Fig. 2b. Major sites where microstructural data were measured during fieldwork are also plotted on the maps of Fig. 2. Differences in structural pattern appear between the two studied areas in space image interpretations and microstructural data. At a regional scale, differences between the eastern and western part of the margin are also reported through the conclusions of previous fieldwork and structural studies carried out, mostly in the eastern (Greenwood and Beackley, 1967; Tard et al., 1991; Thoué, 1993; Thoué et al., 1994; Menzies et al., 1995; Fantozzi, 1996; Insley et al., 1996) and northern (Geukens, 1960; Greenwood and Beackley, 1967; Grolier and Overstreet, 1978; Chiesa et al., 1983; Bohannon, 1989; Menzies et al., 1990, 1992; Huchon et al., 1991; Davison et al., 1994) parts of Yemen. From our work in the southwestern part of the Yemen margin, one can summarise the differences between the Umm Shatt and the Ba'tays areas as follows.

From a stratigraphical point of view:

The Umm Shatt area (Fig. 2a) is characterised by the 2500 m thick Oligo–Miocene Trap Series — so called Yemen Trap Series (Geukens, 1960) — which overlies Cretaceous and Jurassic sedimentary rocks. The Yemen Trap Series consist of volcanic sequences which lie unconformably over Panafrican metamorphic rocks and their Mesozoic cover. Within this sedimentary cover, no angular discordance was found in the field (Thoué, 1993) or in seismic cross-sections (Tard et al., 1991) between Jurassic and Cretaceous deposits. Numerous mafic dikes striking about N130°E intrude the basement and the whole cover in this area.

The Ba'tays area is characterised by thick Jurassic and Cretaceous marl and limestone formations which lie unconformably on the Panafrican basement. Fieldwork shows that the Cretaceous terrains are slightly discordant (about 10°) with the Jurassic formations. This might be due to the Oxfordian deformation depicted along the eastern part of the margin (Tard et al., 1991; Fantozzi, 1996). There is no evidence of volcanic rocks in this area which is located east of the Aden–Dhala transfer zone.

From a structural point of view, tilted blocks can be depicted in both zones:

In the Umm Shatt area (Fig. 2a), tilted blocks (about 2 km wide, 5 km long and dipping about

Fig. 1. (a) Location of the study area. The satellite data are focused on the southern part of the Arabian Peninsula. Large squares correspond to the ground coverage of Landsat TM images (165-51 and 166-51) while small dark-grey shaded squares indicate the location of SPOT images (146-324 and 149-323). (b) Schematic geological map of southern Yemen, modified from Grolier and Overstreet (1978), Tard et al. (1991) and interpretations of Landsat TM images. The two surveyed areas on the southern Yemen margin are indicated wit hblack rectangles.

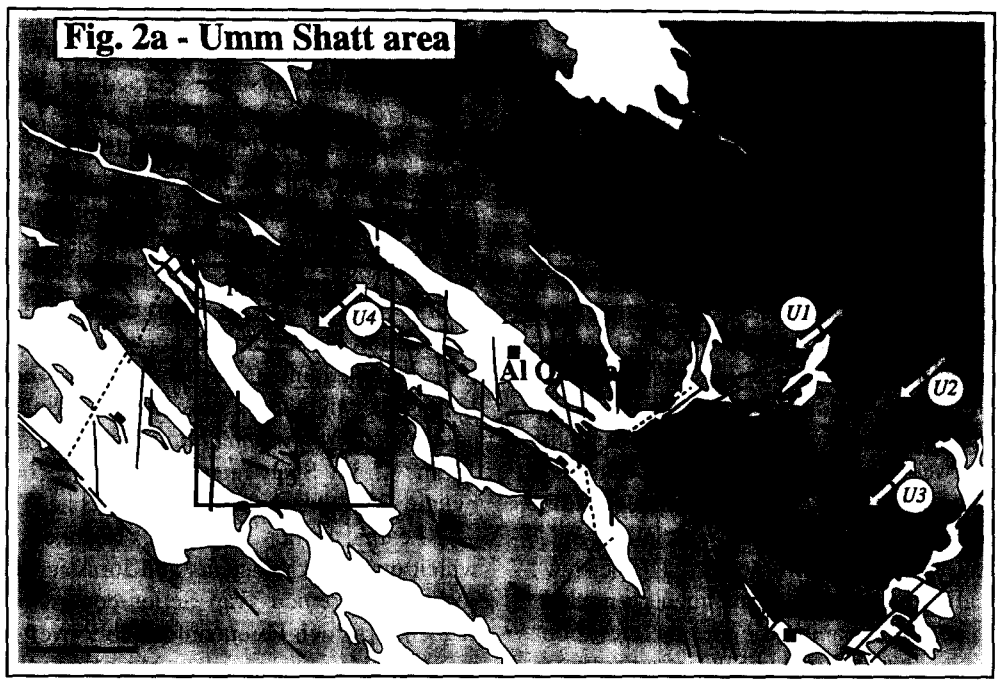
Fig. 2a - Umm Shatt area
U4
U1
U2
U3

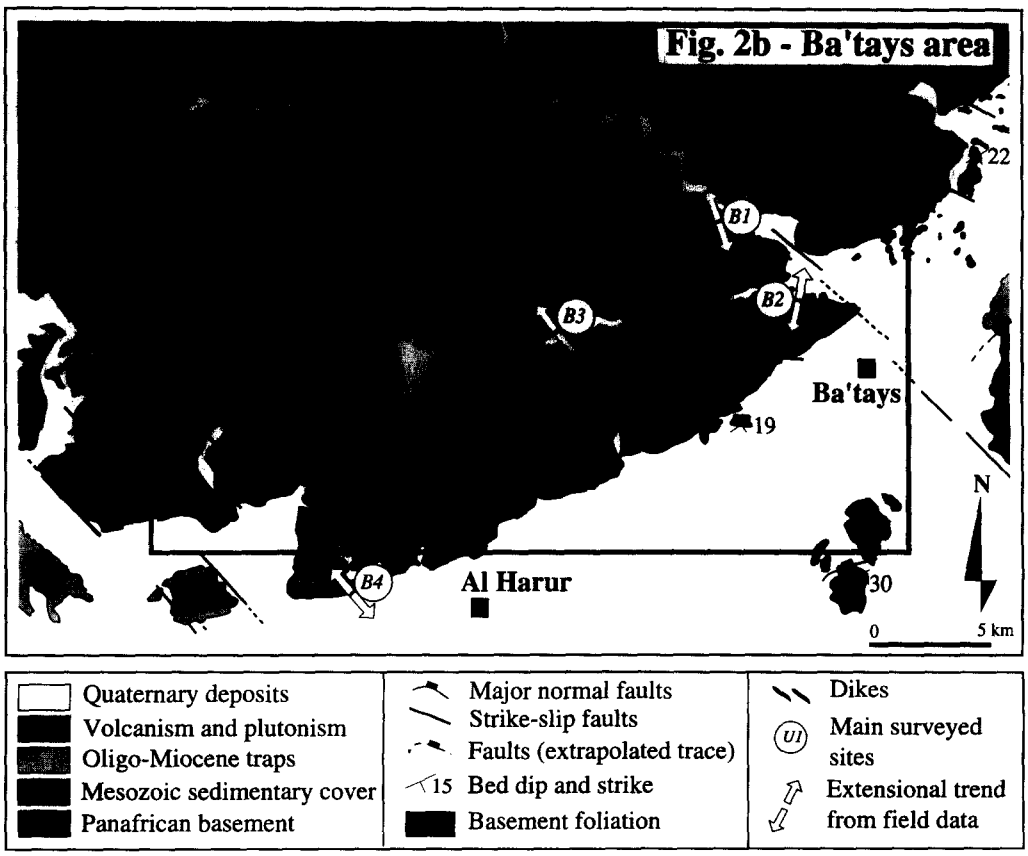
Fig. 2b - Ba'tays area
22
B1
B2
B3
Ba'tays
19
N
B4
Al Harur
30
0
5 km
Quaternary deposits
Volcanism and plutonism
Oligo-Miocene traps
Mesozoic sedimentary cover
Panafrican basement
Major normal faults
Strike-slip faults
Faults (extrapolated trace)
15 Bed dip and strike
Basement foliation
Dikes
U1 Main surveyed sites
Extensional trend from field data

20 degrees southwest toward the Red Sea) are separated by N110°E–N130°E normal faults and N160°E synchronous dextral strike-slip faults. Left-lateral strike-slip faults trending N40°E cut the whole area (Fig. 2a). These faults run parallel to the basement structural trend and to the regional sub-vertical foliation striking about N50°E within this area. These faults might correspond to a basement structure reactivation during extensive phases and they act as limits of the strained area.

In the Ba'tays area (Fig. 2b), tilted blocks are separated by N60°E–N80°E normal faults and from place to place by N140°E right-lateral strike-slip faults. N60°E–N80°E faults are sometimes difficult to identify in the field but can be inferred using satellite images (as broken lines in Fig. 2b suggest) due to a better observation scale. Tilted blocks, dipping about 35 degrees southeast toward the Gulf of Aden, have a greater mean size than those from the Umm Shatt area (about 6 km wide by 25 km long).

3.3. Palaeo-stress reconstruction

The microstructural data were analysed by statistical methods in order to calculate a stress tensor linked to a given population of faults (strike and dip of striations which appear on fault planes). Those methods consist in minimising the angular gap between computed and measured striations (Bott, 1959; Angelier and Mechler, 1977; Carey, 1979; Angelier and Manoussis, 1980; Etchecopar et al., 1981; Angelier, 1983; Gephart and Forsyth, 1984; Michael, 1984). Even if some discussions remain in the case of superimposed tectonic phases (Carey-Gailhardis and Vergely, 1992; Pollard et al., 1993; Nemcock and Lisle, 1995), those methods provide estimations of the local or regional kinematics (Armijo et al., 1982; Carey-Gailhardis and Mercier, 1987). Stress calculations derived from striation measures are expressed in terms of extensional trends, in reference to the least principal stress direction. The results obtained with Michael's calculation method (Michael, 1984) applied to the major measurement sites are plotted on the Schmidt stereonets of Fig. 3 and illustrated by white arrows in Fig. 2. Sites are located in Fig. 2 and referenced by an identification code. As we could observe and as depicted by several authors in western Yemen (Mohr, 1991; Davison et al., 1994) stresses might be locally variable due to plutonism. So, all the measurements were done over areas considered to be representative of regional stresses, in order to avoid as much as possible these local effects on stresses. In the studied areas, several sites make it possible to establish a relative chronology between extensive phases as different striations were measured on the same fault slickensides (Fig. 3).

In the Umm Shatt area, the results point to the existence of a major extensional tectonic phase striking N50°E. This extensional trend is identical to those described in northern Yemen by Huchon et al. (1991) or pointed out by the analysis of dike swarms (Mohr, 1991; Davison et al., 1994). According to several authors (Berhe, 1986; Huchon et al., 1991; Tard et al., 1991) this event occurred in Middle Miocene times.

In the Ba'tays area, the major extensional trend in reference to the least principal stress strikes N135°E. Regarding the chronology of this extensive phase pointed out in the Ba'tays area, even if no precise dating exists, fieldwork shows that all the measured faults affected the whole Mesozoic cover. The N135°E extensive phase appears to be at least of post-Cretaceous times. As no volcanic rocks outcrop in this area and no precise age determinations are available, it might be difficult to compare the kinematics results given by regional stress analysis within the Umm Shatt and Ba'tays sectors. However, those results will be discussed later in this paper, in light of extension calculation, interpretations of displacement fields and regional geological data, in order to precise the chronology of the extensional tectonic events along the southern Yemen margin.

4. Methodology of initial state restoration

In order to obtain the geometry of the initial state of the deformed areas, we propose a method that combines the use of both field structural data and imagery data such as SPOT and Landsat images, DEM

Fig. 2. Detailed structural and geological map of the Umm Shatt (a) and Ba'tays (b) areas. The sectors chosen for geometry modelling indicated with black rectangles.

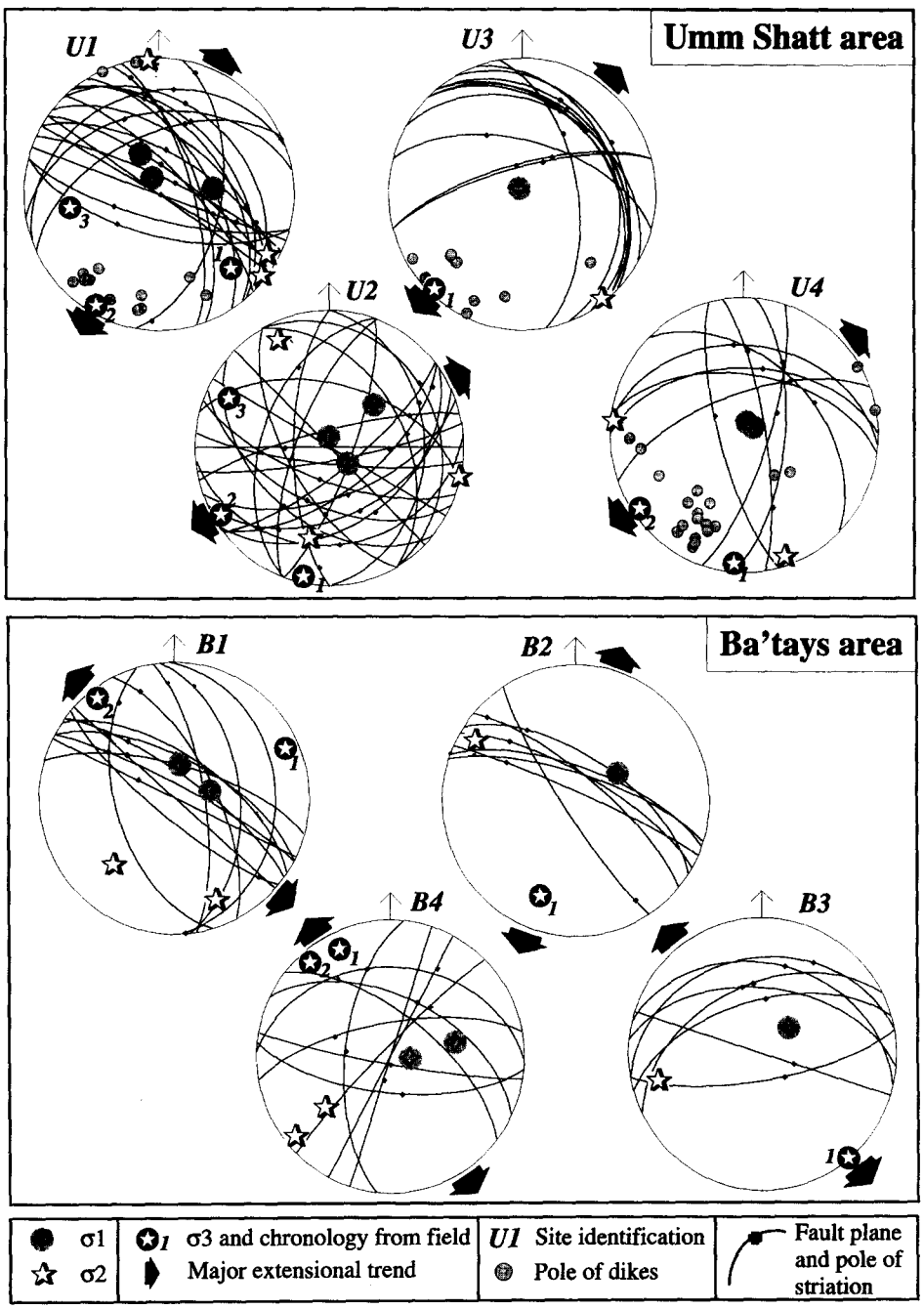

Fig. 3. Stereoplots of the fault data measured at major sites in the Umm Shatt and Ba'tays areas during fieldwork (see location of each site in Fig. 2). Results of stress calculations using Michael's method (Michael, 1984) are plotted as $\sigma 1$, $\sigma 2$ or $\sigma 3$ symbols as well as the relative chronology. Data are plotted on a Schmidt stereonet according to a lower-hemisphere projection.

and 3D perspective views (Thoué, 1993; Thoué et al., 1994; Insley et al., 1996). Thus, we investigated the extension of the southern Yemen margin in several major steps. We (1) choose in the studied area a geological layer as a reference layer, (2) cut its entire faulted surface into several tilted blocks, (3) model

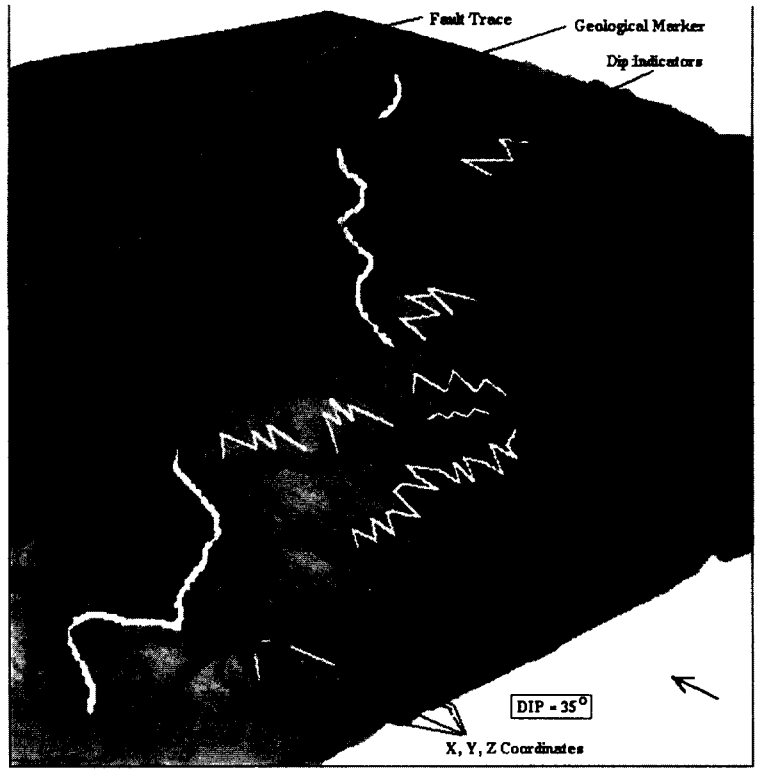

Fig. 4. 3D perspective view focused on the eastern part of the Ba'tays area and built from DEM and SPOT ortho-image combinations. White lines named 'geological marker' correspond to the chosen geological reference layer. Dip indicators are used to determine the strike and dip of exposed geological surfaces. See text. (The small black arrow in the lower right corner of the figure is N-oriented.)

the geometry of the layer within each block, (4) reconstruct the initial state of each tilted block using a restoration method and (5) fit all the restored blocks together to build the initial state of the deformed layer, and (6) estimate the total amount of extension and the finite displacement field, by comparing initial and finite states of the reference layer.

4.1. Choice of a reference layer

In the Umm Shatt area as well as in the Ba'tays area, tilted blocks were identified and a representative sector for the whole area deformation was defined by the combined use of satellite images and field criteria. Each sector is indicated by a rectangle in Fig. 2. The first step consists of identifying a reference layer, that is to say the same geological layer over the entire deformed area. This reference layer is identified on Landsat TM images by its spectral signature and on 3D perspective views by its geomorphologic properties on the fault scarp (Fig. 4). During the field study, the continuity of the geological marker over the whole area was systematically checked and the geomorphologic properties were confirmed. The marker is then used as a strain marker. In the Umm Shatt area, the marker corresponds to a trachytic horizon located in the upper part of the Traps Series. In the Ba'tays area, the marker is a massive calcareous unit forming part of the Lower Jurassic formations (Fig. 4). In both areas, the topmost surface of the marker is used. No thickness variation of each reference layer was recognised in the field.

4.2. 2D mapping of tilted block boundaries

Our method consists in modelling the surface of a geological marker belonging to the tilted blocks rather than the faults separating the blocks, where identification errors may creep in due to the erosion

processes. From the structural maps, we identified several tilted blocks within each studied sector (rectangles in Fig. 2). From Landsat TM images and perspective views, a reference layer was chosen and each tilted block corresponds now to the topmost surface of the geological marker. The 2D mapping of the tilted block boundaries consists of differentiating the area composed by the tilted surfaces of the geological marker from the area composed by the faults. This 2D mapping requires SPOT ortho-images allowing a high ground resolution for definition of tilted block boundaries (ortho-images computed from panchromatic SPOT images with 10 m ground resolution) and a reliable field geological and structural study. According to field observations, two assumptions are made before drawing the boundary of the tilted blocks. First, the erosion is considered to be the same at each point along the margin. Second, a rigid rule of bedding/fault angles is assumed, with an initial dip of the fault plane taken as 60° (Brun and Choukroune, 1983).

Without taking into account the erosion, a part of the tilted block boundary follows the edge of the reference layer that is well-defined by its geomorphologic expression in the fault scarp (Fig. 4). In the theoretical case of block #2 presented in Fig. 5a, this part of the boundary is given by the trace of the geological marker. On the C1–C2 cross-section view (Fig. 5b), this corresponds to point A. However, the fault line joining the two points A and B may verify the assumption concerning the bedding/fault angles. If necessary, this allows one to define a small uncertainty for the exact location of the tilted block boundary due to the eroded part of each tilted block (Fig. 5b).

On the back side of each tilted block, the boundary is more difficult to identify because of the sedimentary filling. Fig. 4c illustrates the uncertainty of the exact position of the fault/marker limit location. Without sedimentary filling (cross-section C1–C2 in Fig. 5b), the location of the fault can be easily detected on the ortho-images. In the C3–C4 cross-section view (Fig. 5c), the boundary of a tilted block still corresponds to point B but different sketches can be drawn from the ortho-images depending on the limits of the sedimentary filling (Fig. 5a and c). Two extreme locations can be defined for the fault trace (points Bl and Bu in Fig. 5c) without any geological sense but that express the uncertainties of the boundary location. These uncertainties which depend on the tilt of the geological markers (blocks 1 and 2), the fault (F) geometry (considered as a plane in this example), the amount of sediment filling and the position of the geological marker in the sedimentary log, may be reduced by a realistic geological drawing on ortho-images and controlled by field data.

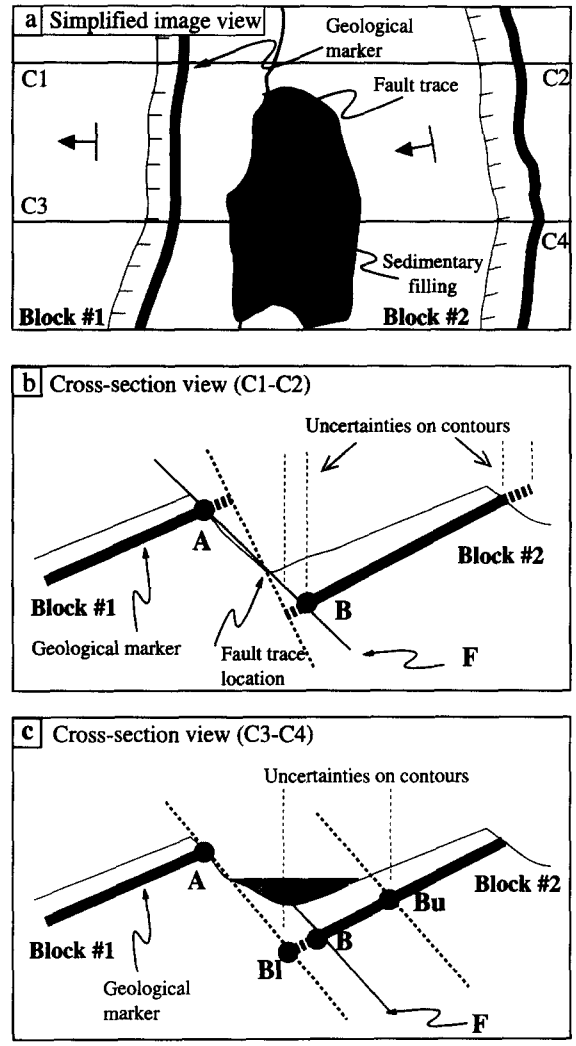

Fig. 5. Identification of deformed block boundaries. The uncertainties are underlined on a map view (or simplified satellite image view) in Fig. 4a and on cross-sections views (Fig. 4b and c).

Finally, the location of the tilted blocks boundary corresponds to the projection of point B (Fig. 5) on an horizontal plane. This boundary is then expressed by numerical (x, y) coordinates. Thirteen and nine

tilted blocks were identified respectively in the Umm Shatt and Ba'tays areas (see Fig. 8a and c for the geometry of the final deformed state).

4.3. Modelling the geometry of the deformed reference layer

We first compute the tilt (strike and dip) of each block of the deformed system directly on the perspective views of each area and check the validity of the numerical measure with field data. Second, we compute the geometry of the topmost surface of the geological marker in order to obtain the numerical model of the whole tilted block system. Before starting the modelling processes, and according to field observations, an other assumption is made, that the reference layer keeps a constant length during strain.

Due to a low vegetation cover and an excellent quality of outcrops in Yemen, dip indicators linked to geological surfaces are clearly visible in the field and easily detectable on 3D perspective views, as underlined by a white strip in Fig. 4. Using the XVOLTER software developed at the Parallelism Computer Science Laboratory (ENS Lyon) it is possible to directly collect on the perspective views the (x, y, z) coordinates of points belonging to the dip indicators exposed on the geological surfaces (bedding planes). For each dip indicator, (x, y, z) coordinates of no less than fifteen constitutive points are determined (Fig. 4). From these coordinates, its strike and dip are computed by a planar regression. A comparison with field measurements shows that no major difference exists with dip computations from perspective views as illustrated in Fig. 6.

In the studied areas, dip measurements are taken on the topmost exposed geological surfaces which do not necessarily correspond to the geological marker itself (Figs. 4 and 5). Each measurement had then to be transposed to the exact depth of the reference layer according to its relative position in the strati-

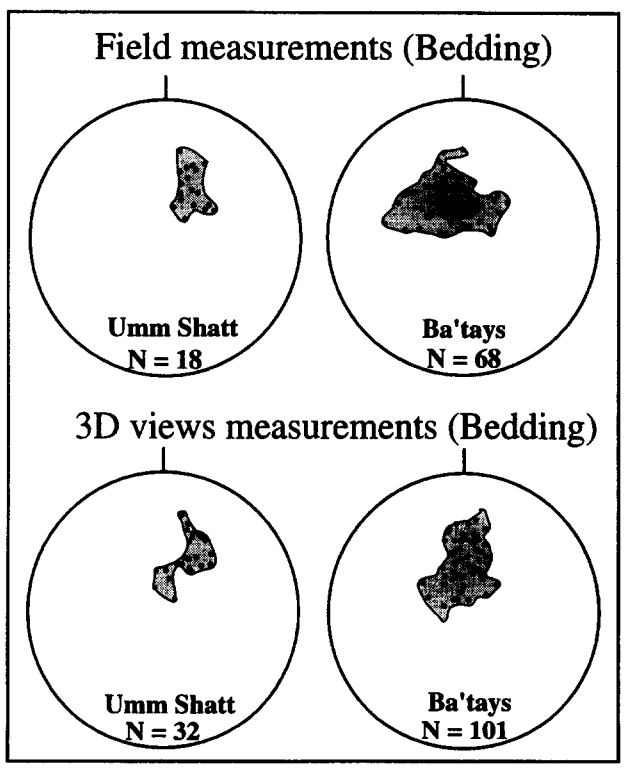

Fig. 6. Comparison between field dip measurements of tilted blocks (upper part of the figure) and computed dips from 3D view coordinates (lower part of the figure). Data from the two areas are plotted on a stereonet using Schmidt projection in the lower hemisphere.

graphic column. This is done assuming a constant thickness of the strata over the entire studied area. As shown by the field survey, tilted blocks differ in the Umm Shatt and the Ba'tays areas (Fig. 2) regarding the structural setting. Two models were so chosen to handle these differences.

In the Umm Shatt sector, the size of the thirteen defined tilted blocks is small. Dip measurements did not show any significant dip variation between the tilted blocks. Thus, in that area, a planar model is used where each tilted block is considered as a plane and rigid. The corresponding numerical model of the reference layer is deduced from only one orientation (strike and dip) determined for each tilted block. The model is then obtained by sampling each tilted block on a common (x, y) mesh where the step (square grid size) is fixed. The z coordinate of each point of the grid is determined over the entire surface of the block, according to the orientation chosen for each tilted block.

In the Ba'tays area, the nine identified tilted blocks are very big. Roll-over structures were evident during fieldwork and major dip variations could be measured from the top, close to the fault scarp, towards the back side of each block. A planar model could not account for these dip variations and a folded model was chosen. According to these variations, all the strike and dip measurements are used to produce the geometrical model of the geological marker surface. As the z coordinates measured from perspective views correspond to the topographic surface (Fig. 4), a new z value is computed for each of the (x, y, z) points assuming a constant thickness of the strata over the entire study area for extrapolation at the depth of the reference layer. The x, y, z coordinates are then interpolated on a Cartesian regular grid using the GMT package (Wessel and Smith, 1991) in order to produce a surface modelling of the reference layer. The choice of such a folded model is clear from Fig. 7 where two profiles are shown across the surface modelling of block #3 of the Ba'tays area (see Fig. 8b for all the tilted block numbers). The initial (L0) and final (L1) lengths are measured for these profiles. The length variation between the deformed state (L1) and the restored (or initial) state (L0) reaches an average value of 20% for the planar model (broken line) and only 3% for the folded model (continuous line). This comparison between L1 and L0 corresponds to a relative shortening with our basic assumption (constant length of the reference layer during strain processes). This example shows the considerable over-estimate on the extensional amount that might be made during the structure restoration procedure, by using a planar model rather than a folded model. Hereafter, the surface modelling of each tilted and folded block of the Ba'tays area is referred to as the 'deformed pieces' in order to distinguish it from the rigid 'tilted blocks' depicted in the Umm Shatt area.

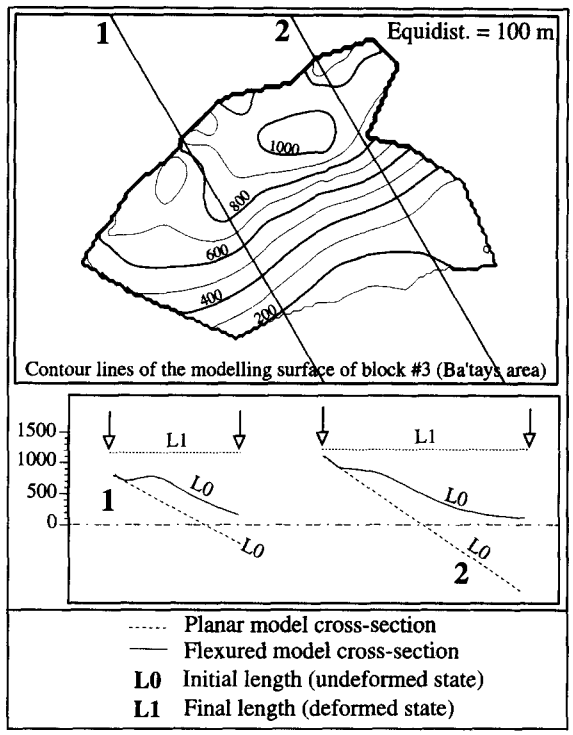

Fig. 7. Appropriateness of the folded model in the Ba'tays area. Contour lines in map view refer to the surface modelling of the geological marker using the folded model and built from computed dip values (see Fig. 3 and text). The cross-section view illustrates the difference between the planar and the folded model of the surface. Dotted lines are obtained by planar approximation from dip data, whereas continuous lines are obtained by approximation with the folded model. L0 corresponds to the initial length of the reference layer, whereas L1 refers to its final length. The ratio L1/L0 is significantly different when using the two interpretations. See Fig. 7 for block 3 location.

Finally, the boundaries that were previously defined for tilted blocks or for deformed pieces (see previous section) are used to limit the surface modelling of each block or piece.

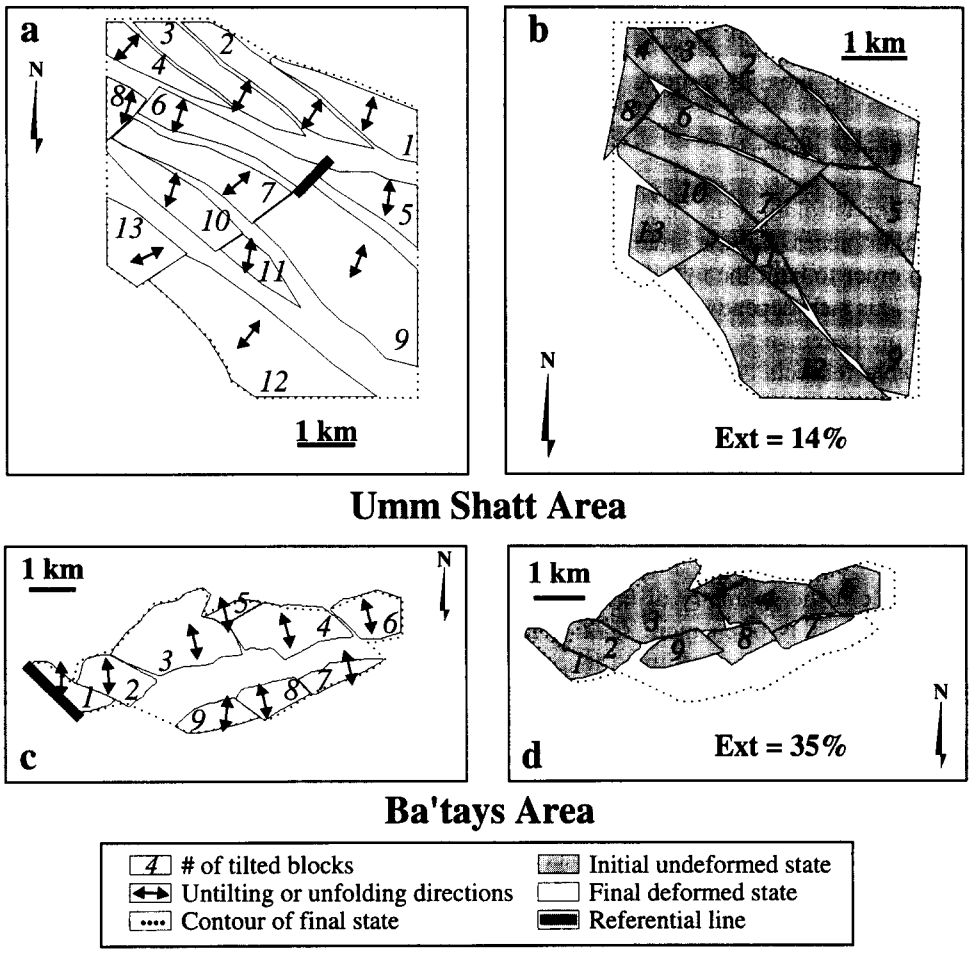

Fig. 8. Models of initial and final states of the two study areas. Fig. 7a and c correspond to the final (present) state in the Umm Shatt and Ba'tays areas, respectively. Arrows represent untilting or unfolding directions deduced from a comparison between deformed and restored states of each block. Fig. 7b and d illustrate the initial (restored) state (after unfolding or untilting and best fitting of the restored blocks). The computed extension is given for the two areas.

4.4. Untilting and unfolding processes

This stage comprises two steps of calculation with either untilting or unfolding procedures depending on the geometry of the reference layers.

In the case of the planar model, each block is individually rotated by its dip angle around its strike in order to find its initial horizontal state. All z coordinates so become identical and we arbitrarily decided they equal 0 assuming no rotation about a vertical axis exist (Thoué, 1993).

In the case of the folded model, the UNFOLD program (Gratier, 1988; Gratier et al., 1991; Gratier and Guillier, 1993) was used to process each deformed piece separately. These pieces are first represented by a network of rigid triangular elements. Each of the deformed pieces is then restored to a horizontal surface, by laying flat the triangular elements. The best fit of each triangular element in the hole defined by its neighbours is obtained by minimising voids and overlaps using a least-square method. The reliability of the geometry of each unfolded surface is tested by the degree of fitting between all the triangular elements (Guillier, 1991; Guillier and Gratier, 1993). Following these rules, all the restored pieces were considered as true developable surfaces

(equivalent to folded and torn sheets of paper). This supposes that the strain process occurs without significant elongation along the folded surface.

4.5. Fitting the restored elements

After untilting or unfolding, the restored blocks (Umm Shatt area) or pieces (Ba'tays area) have to be fitted together in order to built the initial state of the deformed areas. This step depends on the boundary geometry of restored elements. If the geometry of boundary is reliable (especially the fault geometry which is always the most difficult to acquire), voids and overlaps may be minimised (1) automatically using a least-square method (Audibert, 1990; Rouby et al., 1993), or (2) by hand using graphical software able to process vectorial objects (Gratier et al., 1989). If the geometry of boundary is not accurate enough (for example if the geometry of the fault is not very well known), it is often more reliable to use the directions of unfolding or untilting (deduced from a comparison between each deformed and restored element) as indicator for fitting the faults. In the case of the folded model, folding induced by roll-over is related to the displacement of faults. The best compatibility may be established between the directions of unfolding of the deformed pieces and the fault displacements (Gratier and Guillier, 1993), especially in the case where tectonic features correspond to normal or thrust faults.

In both Umm Shatt and Ba'tays areas, displacements of the faults are known (field study) rather better than their geometry. If some common points between two adjacent blocks exist, such as dikes crossing basement and cover, the compatibility between fault displacements (measured in the field) and directions of restoration (untilting or unfolding) is clear. The fault can easily be 'closed' between the two blocks. In other cases (no connected points between blocks), a compromise between both previously exposed rules was sought in order to minimise voids and overlaps between restored blocks, and to match the directions of unfolding and fault displacements. At the end of this step, our method leads to an initial state of the two studied sectors (Fig. 8b and d) that might be compared with the final state of these sectors. Fig. 8 (a and c) illustrates the projection onto a horizontal plane of this final state.

4.6. Extension and displacement fields

The comparison between undeformed (initial) and deformed (final) states gives the amount of extension and allows one to draw the displacement field. For both the Umm Shatt and Ba'tays zones, the extension is calculated as the ratio between the mathematical area of the initial surface and the final surface (Fig. 8). The mathematical area of the final state is determined from the projection of the entire deformed area onto a horizontal plane, including fault gaps and deformed geological surfaces, as illustrated in Fig. 8 (a and c) by dotted lines. The mathematical area of the initial state is drawn following the external boundary of the restored area.

As the initial and final states are known, the finite displacements of each block (represented by the geological marker) can be calculated with respect to a reference (fixed line) chosen within each studied area. In the projection of the final state onto a horizontal plane, the 2D contours of tilted blocks or folded pieces have well-defined (x, y) coordinates. The unfolding and untilting procedures do not produce any change in the number of points which define this contour, so that each set of (x, y) coordinates can be compared between the two states. 2D displacements are defined by the geometrical changes between both initial state and final state and expressed as vectors which are described by a length and an azimuth (see Fig. 9).

4.7. Reliability of the method

To model deformed areas and to compute extension and displacement fields, our method involves the tilted block geometry rather than the fault geometry. Indeed, topographic data yield better constraints on geological surfaces than on their limiting faults (even if fault dips are checked by field measurements). The validity of each step of our method and the accuracy of the amount of extension calculation might be precise. Field arguments have still been discussed regarding the choice of the geological reference layer. No thickness variations nor important internal strain were observed at the scale of each studied area. The main source of errors is in the 2D mapping step. This 2D mapping of tilted block boundaries is directly inferred from the interpretation of satellite ortho-images. Sev-

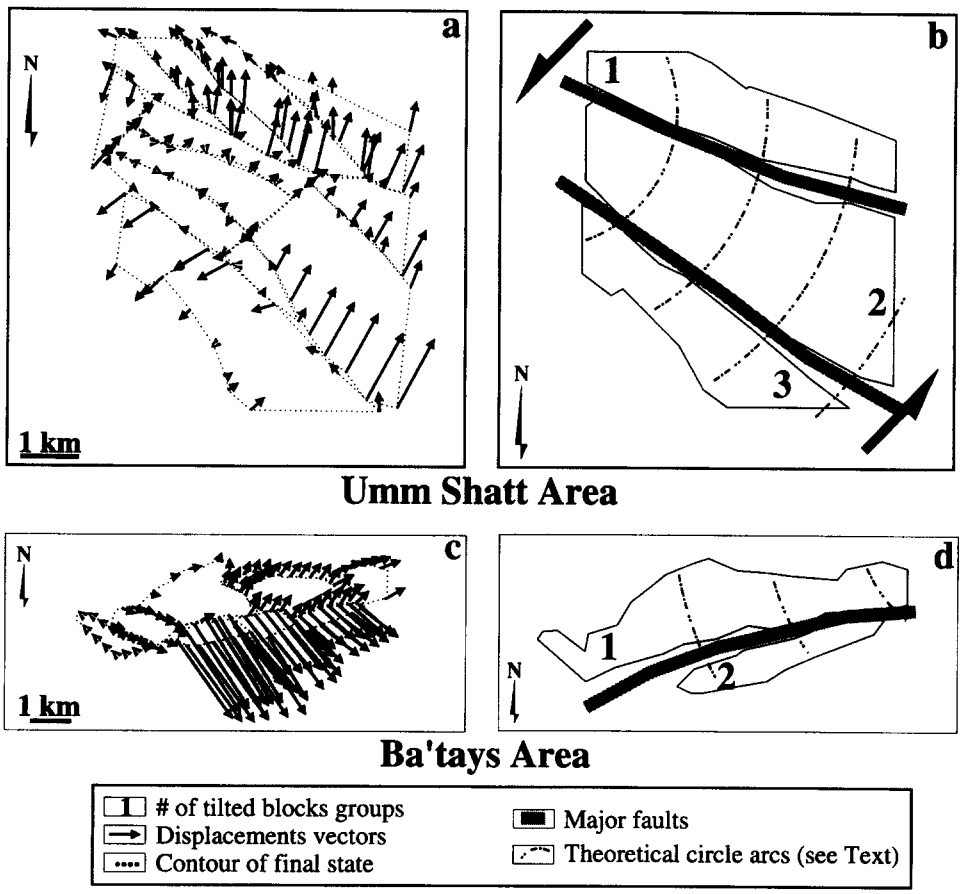

Fig. 9. Total finite displacements vectors drawn from initial (restored) state to final (present) state in the two studied areas. Fig. 8a and c illustrate the displacements field within both areas whereas Fig. 8b and d correspond to an interpretative sketch map of the displacement distribution associated with block rotation and regional shear as indicated by black arrows or dotted lines. See text for explanations.

eral interpretations must be made taking into account the sedimentary filling, the erosion or the errors in fault/marker location. Several configurations corresponding to the final state were tested. Errors linked to this step do not exceed an average of 5% variation in the computed amount of extension (Thoué, 1993). It is also important to notice that the geometrical model (plane or folded) chosen strongly depends on the geological settings of each studied area. The appropriateness of such a model needs to be checked before modelling as we did before by computing length variations in surface modelling (Fig. 7). The interpretation we made from the structural analysis of both the Umm Shatt and Ba'tays sector corresponds to the most realistic structural interpretation and yields a non-unique, but most probable solution, for the initial state reconstruction. Finally, the 2D displacements represent a combination of both continuous and discontinuous strain. So, the displacement fields may vary with the chosen reference layer. However, this method is validated by strictly checking each modelling step with field geological data or structural observations from satellite images. This method can be efficiently used to quantify deformation of the southern Yemen margin.

5. Application to the southern Yemen margin

5.1. Choice of the reference layer

In the Umm Shatt area, fieldwork and microstructural studies reveal that N40°E left-lateral strike-slip

faults are early tectonic features. They might correspond to structures older than the normal faults which separate tilted blocks (Fig. 2a). Their orientation is also sub-parallel to the direction of extension derived from the regional studies and the inversion of fault striations. This implies that no major rotation of these structures would have occurred during strain. Consequently, one of these faults which appears in this area (the eastern limit of block 6, see Fig. 8) was considered as a fixed line.

In the western part of the Ba'tays area, tilted blocks are locally limited by N140°E right-lateral strike-slip faults. These N140°E faults (Fig. 1b) are parallel to the major normal faults that limit the Dhala Graben and cross-cut the whole southern Yemen margin (Tard et al., 1991; Thoué, 1993). The strike of these faults is also close to the N135°E direction of extension determined over this area. According to microstructural evidence in the field, we consider that the N140°E faults act as strike-slip faults during the N135°E extensional event. The N140°E fault which appears on block #1 in the Ba'tays area has been chosen as a fixed line.

5.2. Umm Shatt area

Fig. 8a shows the initial state obtained using the planar model and after fitting each restored block together taking into account fault displacements and/or untilting directions, whether the geometric boundaries of blocks are well-constrained or not. Untilting directions correspond to the major dip of each tilted block as shown by black arrows in Fig. 8a. The distribution of displacement vectors shown in Fig. 9a is obtained with reference to the N40°E fixed line. Vectors are drawn from the initial state to the final state. This distribution can be divided into three distinct zones (zones 1, 2 and 3 in Fig. 9b) separated by N110°E–N130°E faults. As an illustration of the fitting procedure, it may be noticed that blocks in zone 1 (blocks 1, 2, 3 and 4 in Fig. 8a) have been fitted together according mostly to the fault displacements (common points between adjacent blocks), whereas adjacent blocks belonging to different zones (zones 1 and 2 for example) have been fitted together mostly using untilting directions. With such a fitting, the amount of extension over the whole area reaches the value of 14% with a 5% error linked to the computation method as previously described.

Displacement values increase from west to east and are not always parallel to the untilting directions. This is the case along N110°E–N130°E normal faults and is also mostly the case for the N160°E strike-slip faults (northern part of the Umm Shatt area in Fig. 9a). The finite displacement field indicates that the whole area undergoes a sinistral shear. Fig. 9d illustrates an interpretative displacement field that can be drawn by lining up the displacement vectors along segments of circles. These segments of circles may indicate that rotation of tilted blocks along the N110°E–N130°E normal faults could locally accommodate the sinistral shear. These N110°E–N130°E faults may present a slight strike-slip component, as inferred from field data (Figs. 2 and 3). Indeed, field observations and satellite image interpretations locally point out a slight component of dextral strike-slip motion on N110°E–N130°E faults and show a sinistral strike-slip component on all N160°E faults. It may also be noticed that the size of the displacement vectors appears to be different on either side of the N40°E strike-slip fault used as a fixed line. This confirms a posteriori the role of the N40°E pre-existing faults which may guide the block displacements in the Umm Shatt area. Even if the extensional direction is difficult to precisely determine from such a displacements field, it is estimated at around N40°E. The finite displacement field is so compatible with the stress calculations obtained from fault planes and striations analysis, indicating a N50°E extensional tectonic event. This motion is slightly oblique to the system boundaries (N40°E-trending strike-slip faults) and the strike-slip component is locally accommodated by synchronous N160°E strike-slip faults and block rotations (Fig. 2b, Figs. 8 and 9).

5.3. Ba'tays area

Fig. 8c illustrates the initial state of the Ba'tays area built after fitting together restored pieces according to the folded model used to describe blocks in that area. As an example of the fitting procedure, more structural constraints exist on boundaries limiting blocks 1, 2, 3, 4, 5 and 6 rather than on the N60°E–N80°E fault, which limit zones 1 and 2 in Fig. 8d. Over the whole area, the amount of exten-

sion is estimated at 35% (Fig. 8d) with the same 5% methodological error as for the Umm Shatt.

Fig. 9c displays the corresponding displacements field which could be simplified to two zones as pointed out in Fig. 9d. The regional displacement is associated with the relative displacement of blocks belonging to zone 1, versus the blocks of zone 2, along the N60°E–N80°E normal fault. The displacement direction varies from N125°E (eastern part) to N145°E (western part) with an increase of vector length toward the west. In the field, the N60°E–N80°E normal faults may correspond to composites of different trending segments of normal faults separated by small linked strike-slip faults. All these faults develop during an extensional event with a trending direction compatible with the N135°E direction of extension derived from field data analysis (Figs. 2 and 3). As for the Umm Shatt area, we tried to line the displacement vectors up on segments of circles (Fig. 9c). However, from such a simplified interpretation, it is difficult to deduce rotation of tilted blocks along the N60°E–N80°E normal faults as we discuss hereafter.

Indeed, some remarks have to be made regarding the interpretation of the displacements field in the Ba'tays area. Small vectors striking about N30°E–N60°E appear in the northeastern part of the area (Fig. 9c). This orientation could be due to poor constraints on block 6 located on the other side of a N140°E strike-slip fault, which perhaps belongs to another tilted block system, toward the east. The displacement field is also associated with the restoration of one major fault striking N60°E–N80°E. This major limitation means that the extension value is still imprecise and probably over-estimated. This makes the interpretation of displacement fields more questionable especially concerning local rotations which may reflect some local effects rather than being representative of the whole margin. However, inversion of field measurements yields one major extensional trend striking N135°E and matching the computed displacements well.

6. Regional interpretations of the results

With our method combined with several scales of observations, from satellite to field, we could analyse and quantify the deformation and the regional kinematics of a wide part of the southern Yemen margin. We obtained results showing very good agreement between the regional measurements (derived from satellite image interpretations, and geometrical strain modelling) and local measurements (derived from stress tensors computed from field data). In both studied areas, large normal faults present a slight strike-slip component in order to accommodate a regional shear. This strike-slip component yields to small rotations (5–10°) of tilted blocks.

However, our results demonstrate that the studied areas present multiple differences regarding the structural setting as pointed out in Figs. 2, 8 and 9. In the Umm Shatt area, the size and dip of the tilted blocks appear to be smaller than in the Ba'tays area. The major set of faults that limit the tilted blocks strikes N110°E–N130°E and N60°E–N80°E in the Umm Shatt and the Ba'tays sectors, respectively. The computed amount of extension differs too as illustrated in Fig. 8 (b and d). This amount (computed over the entire surface of the areas, see Section 4) is much greater in the Ba'tays area (35%) than in the Umm Shatt area (14%). Our methodology is based on the assumption that no length variation of the reference layer occurs during deformation. This means that the internal strain such as for dikes is not taken into account. In the Umm Shatt area, numerous dikes were depicted during field surveys. Even if the amount of extension might be slightly underestimated in the Umm Shatt area, the part of the extension associated with the dikes could not explain the difference with the Ba'tays area. Regarding the direction of extension determined from fault striation analyses, the major extensive event strikes N50°E in the Umm Shatt area whereas it strikes N135°E in the Ba'tays area (Fig. 2). Finally, the displacement fields indicate two different major directions of displacements in the Umm Shatt and Ba'tays areas, respectively (Fig. 9).

All these differences suggest different kinematics behaviours for these two parts of the Yemen margin. Previous fieldwork (Tard et al., 1991; Thoué, 1993) shows that a N50°E extensional phase affects Oligo–Miocene traps in the Umm Shatt area up to the Dhala area (Fig. 2a). This extensional event is related to the major Miocene extensional phase as depicted by Huchon et al. (1991). However, no volcanic traps are found in the Ba'tays area and beyond a line

going from Aden to Dhala (see previous sections and Fig. 1b; Greenwood and Beackley, 1967; Tard et al., 1991; Menzies et al., 1992, 1995; Thoué, 1993). Consequently, no precise age can be attributed to the N135°E extensional event depicted in the Ba'tays area. The major structures associated with this event affect Cretaceous series and can just be dated as a post-Cretaceous event. But this extensive event does not appear in the Miocene to Recent evolution of the Arabian plate (Gaulier and Huchon, 1991; Jestin and Huchon, 1992). So, all these facts support the existence of two distinct extensional phases, as illustrated by the sketch in Fig. 10, and they are consistent with the existence of several crustal blocks which compose the southern Yemen margin.

The first extensional phase, striking N135°E, would have occurred in Late Cretaceous or Early Miocene times. It is mainly located around the Ba'tays area and more generally in the eastern part of southern Yemen as several authors may indicate (Tard et al., 1991; Menzies et al., 1995; Fantozzi, 1996). This event would appear to be responsible for the development of N60°E–N80°E normal faults and their associated tilted block systems. The latest extensional phase, striking N50°E, occurred during Middle Miocene times (Fig. 10) and affects mostly the entire western and southwestern parts of Yemen (Huchon et al., 1991; Menzies et al., 1992, 1995; Thoué, 1993; Davison et al., 1994), whereas it may disappear toward the east or, alternatively, be still present in other crustal blocks in that direction (Fantozzi, 1996).

Geological observations along the southern Yemen margin argue for the existence of a major transfer zone between both areas, in the northwest of Aden (see Fig. 1b and Fig. 10) (Greenwood and Beackley, 1967; Tamsett, 1984; Tard et al., 1991; Smith, 1993; Thoué, 1993) and for a westward migration of deformation to Afar, during Miocene times (Gaulier and Huchon, 1991; Jestin and Huchon, 1992). The early N135°E phase, evidenced in this paper, could correspond to a preliminary extensional phase, linked to the earlier opening of the Gulf of Aden, and predating the major N50°E extensional event recorded over the whole southeastern part of the Arabian Peninsula. Thus, some complementary structural studies and determination ages are necessary to confirm this interpretation, especially in the area located in the vicinity and eastward of the major graben northwest of Aden (Ad Dhala Graben).

7. Summary

This work pointed out the efficiency of regional structural studies which combine topographic data, digital images, tectonic data and a restoration method. In the southern Yemen stretched margin, this approach makes it possible: (1) to build a geometrical and numerical model of a folded and faulted geological layer, from satellite images, topographic data and field structural data; (2) to restore (by untilting or unfolding) this deformed layer and to fit each restored piece along faults, in order to reconstruct its initial undeformed state; (3) to compare deformed and undeformed states, in order to estimate the amount of extension and the total finite displacement field (relative to a fixed reference) in the two study areas.

Comparison between the computed numerical model of the deformed areas and fieldwork measurements (strike and dip of tilted blocks) shows very good agreement attesting to the reliability of the modelling procedure. The calculations present the first quantification of the amount of extension in the southern Yemen margin. Amounts of extension vary from place to place along this stretched margin. In the Umm Shatt area, Miocene extension reaches 15% with a mean displacement direction corresponding to a N50°E transtensional regime. In the Ba'tays area, post-Cretaceous extension is about 35% with a mean displacement corresponding to a N135°E normal extensional regime.

Comparison between the computed displacement fields and the measured (incremental) displacements (deduced from stress analysis using slickensides inversion) attest to the accuracy of the method. In both areas, normal faults present a small strike-slip component with relative rotation of the blocks (about 5 to 10 degrees) and local accommodation of the extensive strain by synchronous strike-slip faults (mostly in the Umm Shatt area). Most of the methodological uncertainties come from the contouring of the tilted blocks on satellite images, but the use of untilting or unfolding directions and field data as constraints for the fitting procedure of restored blocks greatly

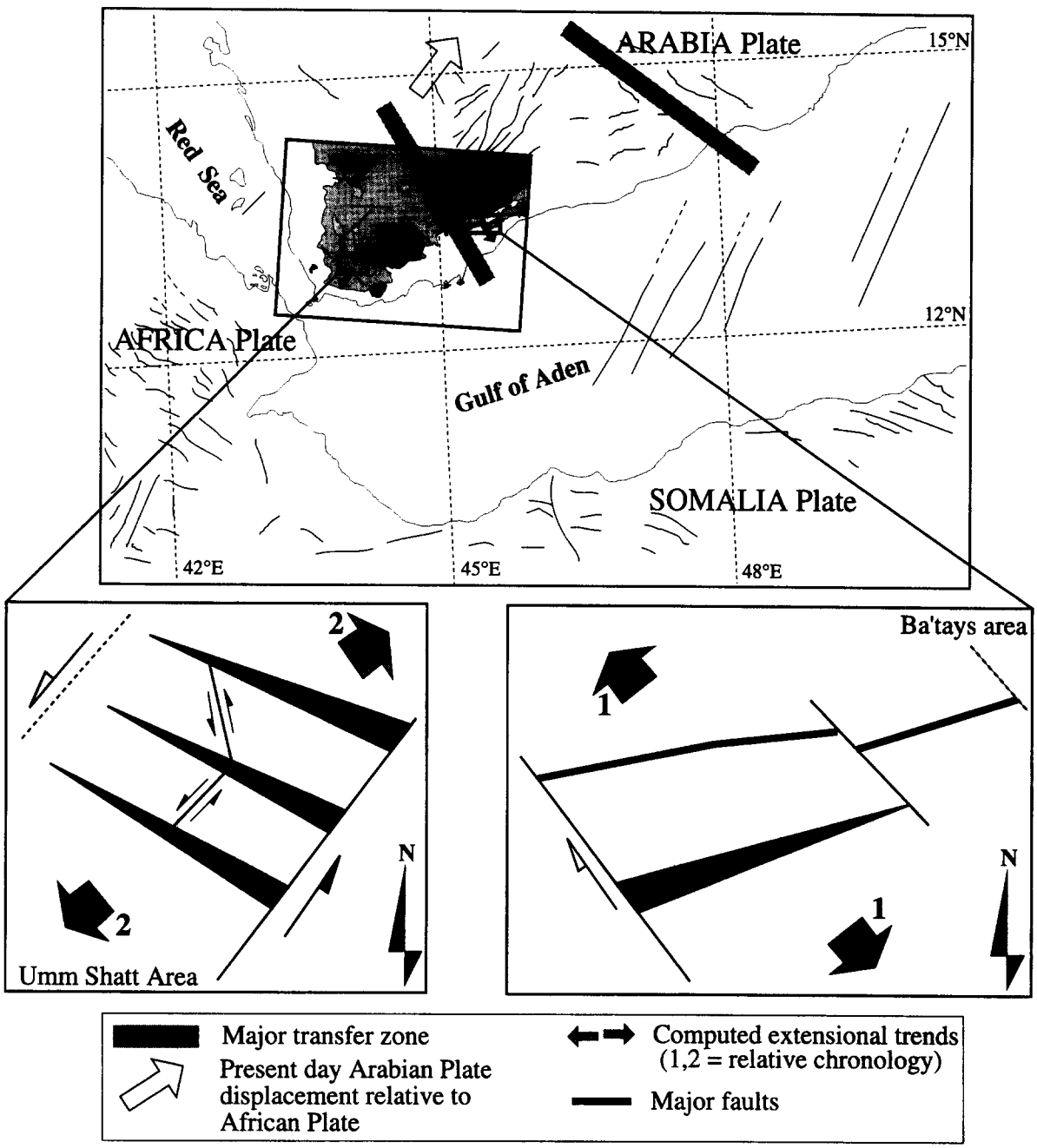

Fig. 10. Local kinematics interpretations of the Umm Shatt and Ba'tays areas replaced in the regional geological and structural context of the African, Arabian and Somali plates triple junction.

improves the coherence between computed models and field measurements.

Finite deformation and displacements suggest an earlier extensional phase which occurred in the northern margin of the Gulf of Aden, even if the detailed chronological timing of those extensional phases in the entire southern margin needs to be confirmed.

Acknowledgements

This work was supported by an INSU and CNRS programme for fieldwork and SPOT image acquisition. Fieldwork and Landsat TM image analysis were facilitated by the logistic help of the Elf-Aquitaine company and J.P. Xavier. We would like to thank M. Mémier, S. Miguet and S. Contassot for the invaluable technical help they provided during this work. Finally, we would also like to thank P. Huchon and an anonymous reviewer for their helpful reviews, which improved this paper.

References

Angelier, J., 1983. Analyses qualitative et quantitative des populations de jeu de failles. Bull. Soc. Géol. Fr. 7, 661–672.

Angelier, J., Manoussis, S., 1980. Classification automatique et distinction des phases superposées en tectonique de failles. C. R. Acad. Sci. Fr. D, 307–310.

Angelier, J., Mechler, P., 1977. Sur une méthode graphique de recherche des contraintes principales, également utilisable en tectonique et sismologie; la méthode des dièdres droits. Bull. Soc. Géol. Fr. 6, 1309–1318.

Armijo, R., Carey, E., Cisternas, A., 1982. The inverse problem in microtectonics and the separation of tectonic phases. Tectonophysics 82, 145–160.

Audibert, M., 1990. Déformation continue et rotations de blocs. Méthodes numériques de restauration. Application à la Galilée. Thèse de 3ème Cycle, Rennes 1, pp. 190.

Barr, D., 1985. 3-D Palinspastic restoration of normal faults in the Inner Moray Firth: implications for extensional basin development. Earth Planet Sci. Lett. 75, 191–203.

Berhe, S.M., 1986. Geologic and geochronologic constraints on the evolution of the Red Sea–Gulf of Aden and Afar Depression. J. Afr. Earth Sci. 5, 101–117.

Bohannon, R.G., 1989. Style of extensional tectonism during rifting, Red Sea, and Gulf of Aden. J. Afr. Earth Sci. 8, 589–602.

Bott, M.H., 1959. The mechanics of oblique slip faulting. Geol. Mag. 96, 109–117.

Brun, J.-P., Choukroune, P., 1983. Normal faulting, block tilting and decollement in a stretched crust. Tectonics 2 (4), 345–346.

Capaldi, G., Manetti, P., Piccardo, G., Poli, G., 1987. Nature and geodynamic significance of the Miocene dike swarm in North Yemen (YAR). Neues Jahrb. Mineral. 2, 207–229.

Carey, E., 1979. Recherche des directions principales de contraintes associées au jeu d'une population de failles. Rev. Geol. Dyn. Geogr. Phys. 21, 57–66.

Carey-Gailhardis, E., Mercier, J., 1987. A numerical method for determining the state of stress using focal mechanisms of earthquakes populations: application to Tibetan teleseisms and microseismicity of Southern Peru. Earth Planet. Sci. Lett. 82, 165–179.

Carey-Gailhardis, E., Vergely, P., 1992. Graphical analysis of fault kinematics and focal mechanisms of earthquakes in terms of stress; the right dihedra method, use and pitfalls. Ann. Tectonicae 6, 3–9.

Chiesa, S., La Volpe, L., Lirer, L., Orsi, G., 1983. Geological and structural outline of Yemen Plateau: Yemen Arab Republic. Neues Jahrb. Geol. Paläontol. Monatsh. 11, 641–656.

Cobbold, P.R., 1979. Removal of finite deformation using strain trajectories. J. Struct. Geol. 1, 67–72.

Cobbold, P., Percevault, M.N., 1983. Spatial integration of strains using finite elements. J. Struct. Geol. 5, 299–305.

Dahlström, C.D.A., 1969. Balanced cross-sections. Can. J. Earth Sci. 6, 743–757.

Davison, I., Blakey, S., Bosence, D., Dart, C., Heaton, R., McClay, K., Nichols, G., Owen, L., Yelland, A., 1994. Geological evolution of the south-eastern Red Sea margin, Republic of Yemen. Geol. Soc. Am. Bull. 106, 1474–1493.

DePaor, D.G., 1988. Balanced sections in thrust belts, Part 1. Construction. Bull. Am. Assoc. Pet. Geol. 72, 73–90.

Etchecopar, A., Vasseur, G., Daignières, M., 1981. An inverse problem in microtectonics for the determination of stress tensors from fault striation analysis. J. Struct. Geol. 3, 51–55.

Fantozzi, P.L., 1996. Transition from continental to oceanic rifting in the Gulf of Aden: structural evidence from field mapping in Somalia and Yemen. Tectonophysics 259, 285–311.

Gaulier, J.M., Huchon, P., 1991. Tectonic evolution of Afar triple junction. Bull. Soc. Géol. Fr. 162, 451–464.

Gephart, J.W., Forsyth, D.W., 1984. An improved method for determining the regional stress tensor using earthquake focal mechanism data: application to the San Fernando earthquake sequence. J. Geophys. Res. 89, 9305–9320.

Geukens, F., 1960. Contribution à la géologie du Yémen. Mém. Inst. Géol. Univ. Louvain 21, 117–180.

Gratier, J.P., 1988. L'équilibrage et la restauration en carte de couches plissées et faillées. In: Gratier, J.P. (Ed.), L'équilibrage des coupes géologiques: but, méthodes et applications. Mémoires du CAESS 20, 145–158.

Gratier, J.P., Guillier, B., 1993. Compatibility constraints on folded and faulted strata and calculation of total displacement using computational restoration (UNFOLD program). J. Struct. Geol. 15, 391–402.

Gratier, J.P., Ménard, G., Arpin, R., 1989. Strain-displacement compatibility and restoration of the Chaines Subalpines of the Western Alps. In: Coward, M.P., Dietrich, D., Park R.D. (Eds.), Alpine Tectonics. Geol. Soc. 45, 29–41.

Gratier, J.P., Guillier, B., Delorme, A., Odonne, F., 1991. Restoration and balance of a folded and faulted surface by best-fitting of finite elements: principle and applications. J. Struct. Geol. 13, 111–115.

Greenwood, J.E.G.W., Beackley, D., 1967. Geology of the Arabian peninsula, Aden Protectorate. U.S.Geol. Surv. Prof. Pap. 560-C, 1–95.

Grolier, M.J., Overstreet, W.C., 1978. Geological map of the Yemen Arabic Republic (Sana'a). ASGS Misc. Inv. Series.

Guillier, B., 1991. Dépliage automatique de strates plissées et faillées. Application à l'équilibrage de structures naturelles. Thèse de 3ème Cycle, Univ. Grenoble 1, pp. 161.

Guillier, B., Gratier, J.P., 1993. Dépliage automatique de surfaces: tests de la géométrie des strates plissées. C.R. Acad. Sci. Paris 313, 1313–1318.

Hossack, J.R., 1979. The use of balanced cross-sections in the calculation of orogenic contraction: A review. J. Geol. Soc. London 136, 705–711.

Huchon, P., Jestin, F., Cantagrel, J.M., Gaulier, J.M., Al Khirbash, S., Gafaneh, A., 1991. Extensional deformations in Yemen since Oligocene and the Africa–Arabia–Somalia triple junction. Ann. Tectonicae 5, 141–163.

Insley, M.W., Murphy, F.X., Naylor, D., Critchley, M., 1996. The use of satellite imagery in the validation and verification of structural interpretations for hydrocarbon exploration in Pakistan and Yemen. In: Buchanan, P.G., Nieuwland, D.A. (Eds.), Modern Developments in Structural Interpretation, Validation and Modelling. Geolog. Soc. Spec. Publ., London, pp. 321–343.

Jestin, F., Huchon, P., 1992. Cinématique et déformation de la jonction triple Mer Rouge–Golfe d'Aden–Rift éthiopien depuis l'Oligocène. Bull. Soc. Geol. Fr. 163, 354–361.

Mc Coss, A., 1988. Restoration of transpression/transtension by generating the three-dimensional segmented helical loci of deformed lines across structure contour map. J. Struct. Geol. 10, 109–120.

Mémier, M., 1991. Stéréophotogrammétrie numérique: calcul de MNT par corrélation automatique d'images SPOT. Thèse de 3ème Cycle, Univ. Grenoble 1, 154 pp.

Ménard, G., 1987. Structure et cinématique d'une chaine de collision: les Alpes occidentales et centrales. Thèse d'Etat, Grenoble 1, 260 pp.

Menzies, M., Bosence, D., El-Nakhal, H.A., Al-Khirbash, S., Al-Kadasi, M., Al Subbary, A., 1990. Lithospheric extension and the opening of the Red Sea: sediment–basalt relationships in Yemen. Terra Nova 2, 340–350.

Menzies, M.A., Baker, J., Bosence, D., Dart, C., Davidson, I., Hurford, A., Al'Kadasi, M., McClay, K., Nichols, G., Al'Subbary, A., Yelland, A., 1992. The timing of magmatism, uplift and crustal extension: preliminary observations from Yemen. In: Storey, B.C., Alabaster, T., Pankhurst, R.J. (Eds.), Magmatism and the Causes of Continental Break-Up. Geol. Soc. London 68, 293–304.

Menzies, M., Al-Kadasi, M., Al-Khirbash, S., Al-Subbary, A., Baker, J., Blakey, S., Bosence, D., Davison, I., Dart, C., Owen, L., McClay, K., Nichols, G., Hurford, A., Yelland, A., Watchorn, F., 1995. Geology of Yemen. In: Ministry of Oil and Mineral Resources (Eds.), Geology and Mineral Resources of Yemen, pp. 21–48.

Michael, A.J., 1984. Determination of stress from slip data: faults and folds. J. Geophys. Res. 89, 11517–11526.

Mohr, P., 1991. Structure of Yemeni Miocene dike swarms, and emplacement of coeval granite plutons. Tectonophysics 198, 203–221.

Moseley, F., 1969. The Aden traps of Dhala, Musaymir and Radfan, South Yemen. Bull. Volcanol. 33, 889–909.

Mugnier, J.L., Arpin, R., Thouvenot, F., 1987. Coupes équilibrées à travers le massif subalpin de la Chartreuse. Geodin. Acta 1, 125–137.

Nemcock, M., Lisle, R.J., 1995. A stress inversion procedure for polyphased fault/slip data sets. J. Struct. Geol. 17, 1445–1453.

Oertel, G., Ernst, W.G., 1978. Strain and rotation in a multilayered fold. Tectonophysics 48, 77–106.

Percevault, M.N., Cobbold, P.R., 1982. Mathematical removal of regional ductile strains in Central Brittany: evidences for wrench tectonics. Tectonophysics 82, 317–328.

Pollard, D.D., Saltzer, S.D., Rubin, A.M., 1993. Stress inversion methods: are they based on faulty assumptions?. J. Struct. Geol. 15, 1045–1054.

Rouby, D., Cobbold, P.R., Szatmari, P., Demercian, S., Coelho, D., Rici, J.A., 1993. Least-squares palinspastic restoration of regions of normal faulting — application to the Campos basin (Brazil). Tectonophysics 221, 439–452.

Schultz-Ela, D.D., 1988. Application of a three-dimensional finite-element method of strain field analyses. J. Struct. Geol. 10, 263–272.

Schwerdtner, W.M., 1977. Geometric interpretation of regional strain analysis. Tectonophysics 39, 515–531.

Smith, J.V., 1993. Infinitesimal kinematics of rotational rifting with reference to en echelon marginal faults in the Red Sea region. Tectonophysics 222, 227–235.

Tamsett, D., 1984. Comments on the development of rifts and transform faults during continental break-up; examples from the Gulf of Aden and Northern Red Sea. Tectonophysics 104, 35–46.

Tard, F., Masse, P., Walgenwitz, F., Gruneisen, P., 1991. The volcanic passive margin in the vicinity of Aden, Yemen. Bull. Cent. Rech. Explor. Prod. Elf Aquitaine 15, 1–9.

Thoué, F., 1993. Quantification par imagerie tridimensionnelle de l'extension continentale et des déplacements associés. Exemples au Kenya et au Yémen. Thèse de 3ème Cycle, Univ. J. Fourier, Grenoble 1.

Thoué, F., Vidal, G., Gratier, J.P., 1994. Quantification par imagerie 3D d'un champ de déplacements sur la marge Sud du Yémen: implications sur l'ouverture du Golfe d'Aden. C.R. Acad. Sci. Paris, Sér. II 319, 825–832.

Wessel, P., Smith, W.H.F., 1991. Free software helps map and display data. EOS, Trans. Am. Geophys. Union 72, 445–446.